Numerical study of gain equalization in burst-mode Yb^{3+}-doped fiber amplifier with pulse pump by FDTD method*

ZHU Longfei (朱龙飞), **LI Caiyun** (李彩云), **LIU Yange** (刘艳格), **XING Dengke** (邢登科), **ZHANG Luhe** (张露鹤), **ZHU Kaiyan** (朱开颜), **and WANG Zhi** (王志)**

Tianjin Key Laboratory of Optoelectronic Sensor Sensing Network Technology, Institute of Modern Optics, Nankai University, Tianjin 300350, China

(Received 24 November 2020; Revised 14 December 2020)

The amplifying dynamics of the pulse burst in Yb^{3+}-doped fiber amplifier (YDFA) with high-power pulse pump is numerically analyzed by a finite-difference time-domain (FDTD) method. The numerical simulations show that the amplitude uniformity of the amplified pulse burst can be modified by adjusting the parameters of pump, such as relative delay and power. Though optimizing the pump parameters, we can reduce the gain difference between the pulses in a burst and improve the efficiency of coherent pulse stacking based on Gires-Tournois interferometers (GTIs). These results can be applied to the design of high energy ultra-short pulse amplifiers based on burst-mode amplification and coherent pulse stacking technology.

Document code: A **Article ID:** 1673-1905(2021)08-0496-5

DOI https://doi.org/10.1007/s11801-021-0189-0

Ultrafast laser with high peak power has very important applications in industrial processing, biomedicine, military defense and other fields[1,2]. Compared with the huge volume and efficiency of solid-state lasers, fiber lasers have the advantages of stability, flexible structure, beam quality and high efficiency. However, detrimental nonlinear effects and optical damage induced by thermal effects in fiber limit the further increase of the peak power. In order to obtain high-energy, high-repetition ultrafast pulses, while reducing the impact of thermal effects, burst-mode fiber amplification technology has attracted widespread attention. In this architecture, each burst contains a certain number of pulses with a repetition rate ranging from hundred megahertz to gigahertz, and the repetition rate of the bursts can be as low as kilohertz[3-8]. Kalaycioglu et al[3,5] firstly demonstrate fiber burst-mode amplifier system based on polarization-maintaining Yb-doped fibers and 1 mJ burst energy was achieved with 1 kHz burst repetition frequency. In 2012, Breitkopf et al[4] showed 58 mJ burst energy burst amplifier based on an Ytterbium-doped large-pitch fiber. In 2015, Kalaycioglu et al[9] reported a burst mode polarization maintaining YDFA system pumped by synchronous pulse, and obtained 1 040 nm pulse burst output with pulse burst repetition rate of 1 kHz, inter burst pulse repetition rate of 100 MHz, total pulse energy of 400 μJ and single pulse energy of 40 μJ. In 2018, Yu et al[10] reported a burst-mode fiber amplifier with burst energy 8.3 mJ and average power 166 W. In 2020, Yang Zhongmin et al[7] reported an all fiber YDFA system with femtosecond pulse bursts and obtained pulse burst outputs with pulse burst repetition rate of 1 MHz, inter burst pulse repetition frequency of 1.2 GHz and average power of more than 100 W. Nowadays, the burst-mode fiber laser system have used in material processing[11], photoacoustic microscopy[12], pulsed laser deposition[13], and mid-infrared optical parametric oscillator[14].

Recently, the combination of burst-mode fiber amplifier and pulse stacking technology provides a new solution for realization of high-energy ultrashort pulses[15-19]. Galvanauskas et al[15] proposed and demonstrated coherent pulse stacking amplification (CPSA) in 2015, which can transform a sequence of pulses coherently in reflecting resonators cavities, e.g. Gires-Tournois interferometers (GTIs), into a single output pulse. The pulse energy output from the GTI-based CPSA is sensitive to sub-pulse amplitudes. The different sub-pulse amplitudes will seriously affect the efficiency of pulse stacking. The homogenous pulses can be achieved by compensating the burst envelope distortion before amplification[7]. However, it is difficult to obtain homogenous pulses for multi-stage fiber amplifier with high gain because the pulse amplification is a nonlinear process. In order to suppress amplified spontaneous emission (ASE) between the bursts at low inter-burst repetition rate, synchronously pulsed pump usually adopt in burst-mode fiber amplifi-

* This work has been supported by the National Key Research and Development Program of China (No.2018YFB0504400), the National Natural Science Foundation of China (Nos.61775107, 11674177, 61640408) and the Tianjin Natural Science Foundation (No.19JCZDJC31200).
** E-mail: zhiwang@nankai.edu.cn

er[20]. Therefore, the homogenous pulses can be achieved by controlling the relative position of the pump pulse and burst.

In this paper, we present a theoretical analysis on the burst-mode YDFA with pulse pump by an FDTD Method. The dynamic characteristics during the amplification of nanosecond pulse burst with kilohertz repetition rates, such as the average gain and the amplitude uniformity of the pulse burst, are compared under different conditions. The homogenous pulses can be achieved by controlling signal delay time and pump pulse power and duration. The impacts of the output pulse energy and the efficiency of coherent pulse stacking from the amplitude uniformity of the amplified pulse burst are also discussed.

The schematic diagram of burst-mode YDFA with pulse pump and time pulse stacking system is presented in Fig.1, which uses a large-mode-area polarization maintain ytterbium-doped photonic crystal rod-type fiber (DC-200/70-PM-Yb-ROD) to suppress detrimental nonlinear effects and achieve high energy output. The coherent pulse stacking system which is composed of 4 GTI cavities can stack 25 pulses coherently into a pulse.

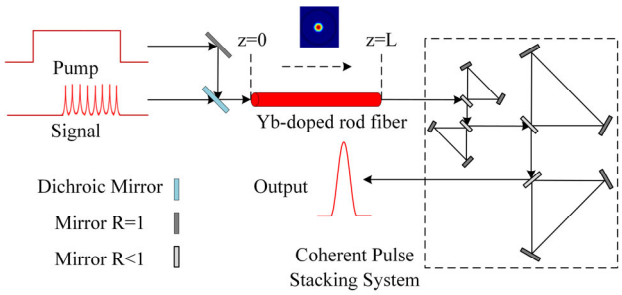

Fig.1 Schematic diagram of a burst-mode YDFA with pulse pump and time pulse stacking system

The rate equations for the YDFA are given by[21]

$$N = N_1 + N_2 , \tag{1}$$

$$\frac{\partial N_2}{\partial t} + \frac{N_2}{\tau} = \frac{\Gamma_p \lambda_p}{hcA}\left[\sigma_{ap} N_1 - \sigma_{ep} N_2\right] P_p + \frac{\Gamma_s \lambda_s}{hcA}\left[\sigma_{as} N_1 - \sigma_{es} N_2\right] P_s , \tag{2}$$

$$\frac{\partial P_p}{\partial z} + \frac{1}{v_p}\frac{\partial P_p}{\partial t} = \Gamma_p\left[\sigma_{ep} N_2 - \sigma_{ap} N_1\right] P_p - \alpha_p P_p , \tag{3}$$

$$\pm\frac{\partial P_s}{\partial z} + \frac{1}{v_s}\frac{\partial P_s}{\partial t} = \Gamma_s\left[\sigma_{es} N_2 - \sigma_{as} N_1\right] P_s - \alpha_s P_s + 2\sigma_{es} N_2 \frac{hc^2}{\lambda_s^3}\Delta\lambda_s , \tag{4}$$

where N is the total concentration of Yb^{3+}, N_1 and N_2 are the lower and upper level population concentrations, respectively; P_p and P_s are pump power and signal power, respectively; Γ_p and Γ_s are the power overlapping factors between the pump and signal and the Yb^{3+}-doped fiber area, respectively; A is the doped area; v_p and v_s are the group velocity of the pump and signal, respectively; λ_p and λ_s are the pump and signal wavelengths, respectively; α_p and α_s are the fiber attenuation coefficient of the pump and signal powers, respectively; h and c is the Planck constant and the speed of light in vacuum, respectively; σ_{ap} and σ_{as} are the absorption cross sections of the pump and the signal powers, respectively; σ_{ep} and σ_{es} are the emission cross sections of the pump and the signal powers, respectively; τ is the fluorescence lifetime; $\Delta\lambda_s$ is the signal band duration. The partial differential Eqs.(1)— (4) are solved using a FDTD method.

$$N_2(k,l+1) = \left[1 - \frac{\Delta t}{\tau} - \frac{\Gamma_p \lambda_p}{hcA}\left(\sigma_{ap} + \sigma_{ep}\right)\Delta t P_p(k,l) - \frac{\Gamma_s \lambda_s}{hcA}\left(\sigma_{as} + \sigma_{es}\right)\Delta t P_s(k,l)\right] N_2(k,l) + \frac{\Gamma_p \lambda_p}{hcA}\sigma_{ap}\Delta t N P_p(k,l) + \frac{\Gamma_s \lambda_s}{hcA}\sigma_{as}\Delta t N P_s(k,l) , \tag{5}$$

$$\left(2\Delta t + \frac{1}{v_p}\Delta z\right) P_p(k+1,l+1) = \frac{1}{v_p}\Delta z P_p(k+1,l-1) + \Delta t P_p(k,l+1) + P_p(k,l)\left\{2\Delta t\Delta z\Gamma_p\left[\left(\sigma_{ep} + \sigma_{ap}\right) N_2(k,l) - \sigma_{ap} N\right] + \Delta t - 2\Delta t\Delta z\alpha_p\right\} , \tag{6}$$

$$\left(2\Delta t + \frac{1}{v_s}\Delta z\right) P_s(k+1,l+1) = \frac{1}{v_s}\Delta z P_s(k+1,l-1) + 4\Delta t\Delta z\sigma_{es} N_2 \frac{hc^2}{\lambda_s^3}\Delta\lambda_s + \Delta t P_s(k,l+1) + P_s(k,l)\left\{2\Delta t\Delta z\Gamma_s\left[\left(\sigma_{es} + \sigma_{as}\right) N_2(k,l) - \sigma_{as} N\right] + \Delta t - 2\Delta t\Delta z\alpha_s\right\} , \tag{7}$$

where k and l are the space and time steps, respectively.

The GTI-based CPSA can stack a sequence of pulses coherently into a single output pulse by using a series of cascaded cavities. Each cavity is comprised of a partially reflecting front mirror and several high-reflectivity mirrors. As shown in Fig.2, at the front mirror M, the initial input pulses $\tilde{A}_n^{in}$ (n= 1, 2, 3,…, N–1) and the pulse $\tilde{A}_{n-1}^{cav.}$ in the cavity interfere destructively at the output port of the cavity, so that energy is stored in the cavity. Then, the final input pulse and the pulse in the cavity interference constructively at the output port, so that all energy is exported from the outside of the cavity into a single pulse. This interference process can be described by the following matrix:

$$\begin{bmatrix} \tilde{A}_n^{out} \\ \tilde{A}_n^{cav.} \end{bmatrix} = \begin{bmatrix} 1 & 0 \\ 0 & \alpha\cdot e^{i\delta} \end{bmatrix} \cdot \begin{bmatrix} r & it \\ it & r \end{bmatrix} \cdot \begin{bmatrix} \tilde{A}_n^{in} \\ \tilde{A}_{n-1}^{cav.} \end{bmatrix} , \tag{8}$$

where r and t are the reflection and transmission coefficients of the mirror M (r^2+t^2=1) and the reflectivity R=r^2, α is the pulse transmission loss and δ is the phase difference of the pulse propagating in the cavity for one cycle.

Theoretical and experimental results show that 2m+1 equal amplitude pulses can be stacked into one pulse

using m concatenated cavities of equal length which forms a "stacking stage". The input pulse sequence of the next stage is composed of the output pulse of the previous stage. The cavity length of the next stage is $2m+1$ times longer than that in the previous stage. A cascaded, k-stage stacking scheme, with m cavities in each stage, in which $(2m+1)^k$ equal-amplitude pulses can be stacked into one pulse[15,18,19].

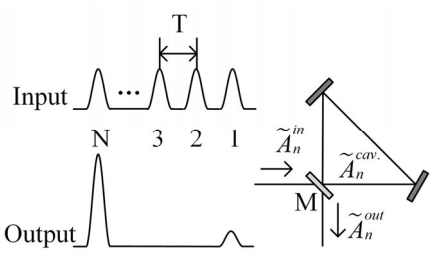

Fig.2 Schematic diagram of coherent pulse stacking based on GTI cavity

The schematic diagram of burst-mode YDFA with pulse pump is presented in Fig.1. The signal is set as a pulse burst composed of 25 Gaussian pulses with peak power of 10 kW, half duration of 0.5 ns and repetition rate of 333 MHz and the pump pulse as rectangular. Meanwhile, the repetition rates of the pump pulse and the signal pulse burst are both 1 kHz. Then they are coupled into the Yb^{3+}-doped rod-type photonic crystal fiber by space coupling. The amplified pulse burst is transformed into one pulse used the coherent pulse stacking system. The main parameters used in the simulations are listed in Tab.1. The value of Γ_s is calculated by using COMSOL to simulate the gain fiber (DC-200/70-PM-Yb-ROD). And Γ_p is simplified as the ratio of doped area to inner cladding area.

Tab.1 Main parameters used in the simulations

Parameter	Value	Parameter	Value
λ_p	976 nm	σ_{as}	2×10^{-27} m^2
λ_s	1 030 nm	σ_{es}	7×10^{-25} m^2
A	3.85×10^{-9} m^2	α_p	0
N	5×10^{25} m^{-3}	α_s	0
τ	1 ms	$\Delta\lambda_s$	2 nm
L	0.8 m	Γ_s	0.999 3
σ_{ap}	2.7×10^{-24} m^2	Γ_p	0.122 5
σ_{ep}	2.7×10^{-24} m^2		

By controlling the delay of pump and signal, we can change the gain of the front and back edge of the pulse burst. But the maximum difference in pulse intensity always occurs between the first pulse and the last pulse. Therefore, in order to analyze the amplitude uniformity of the amplification pulse burst quantitatively, the gain difference is defined as the difference between the gain of the first pulse and the last pulse in the pulse burst. Positive and negative gain differences indicate that the gain of the front edge pulse is higher than and lower than that of the back edge pulse, respectively. When the gain difference is 0 dB, the amplitude uniformity is the best. Fig.3 shows the variation of the gain difference and the average gain of the pulse burst under different signal delay time when the pump power is constant (repetition rate is 1 kHz, pulse duration is 200 ns and peak power is 50 kW). The high peak power pump pulses can be achieved by using a Q-switching fiber laser[22]. The signal delay time is defined as the time interval when the front edge of the pump pulse is ahead of the center of the first pulse in the signal pulse burst. As shown in Fig.3(a), with the increase of delay time, the gain difference and the average gain of the pulse burst increase all the time. When the delay time is less than 67 ns, the gain difference is less than 0, indicating that the gain of the front edge is less than the back edge of the pulse burst. And it can be seen from Fig.3(b) and (c), because Yb^{3+}-doped fiber is not fully pumped, the gain of front edge pulse is low, where delay time is 25 ns. When the delay time is 67 ns, the gain difference is −0.02 dB indicating that the gains of the pulse burst are approximately equal. And it can be seen from Fig.3(d) and (e), where the delay time is 67 ns. When the delay time is more than 67 ns, the gain difference is more than 0, indicating that the front pulse gain of the pulse burst is more than the back edge. And it can be seen from Fig.3(f) and (g), because the front edge pulse exhausts more energy, resulting in higher power of the front edge pulse, where the delay time is 85 ns.

The pump power also affects the amplification of the pulse burst. Fig.4 shows the variation of the gain difference and the average gain of the pulse burst under different pump power when signal delay time is fixed at 50 ns. As shown in Fig.4(a), with the increase of pump power, the average gain of the pulse burst increases all the time. However, the gain difference decreased firstly then increased with increment of pump power. When the pump power is low, the overall gain is small, so the absolute value of gain difference is also small. With the increase of pump power, the overall gain of pulse burst gradually increases, and the absolute value of gain difference also gradually increases. When the pump power is 32 kW, the gain difference reaches the minimum. Then with the increase of pump power to 77 kW, the absolute value of gain difference gradually decreases. At this time, the gain difference is less than 0 dB, indicating that the gain of the front edge of the burst is less than that of the back edge. And it can be seen from Fig.4(b), where the pump power is 30 kW. When the pulse power is 77 kW, the gain difference is −0.03 dB and the uniformity is the best, and it can be seen from Fig.4(d). When the pump power is more than 77 kW, the gain difference is more than 0 dB, indicating that the front pulse gain of the pulse burst is more than the back edge. And it can be seen from Fig.4(f), because the front edge pulse exhausts

more energy, resulting in higher power of the front edge pulse, where the pump power is 100 kW.

Then we numerically simulate the stacking process of the amplified pulse burst in a 2+2 cascade GTI cavity stacker. To analyze the stacking characteristics quantitatively, the stacking efficiency is defined as $\eta=E_{out}/\sum_n E_n$, where E_{out} is the output pulse (stacked pulse) energy and E_n is input pulse energy for n=1,2,…N.

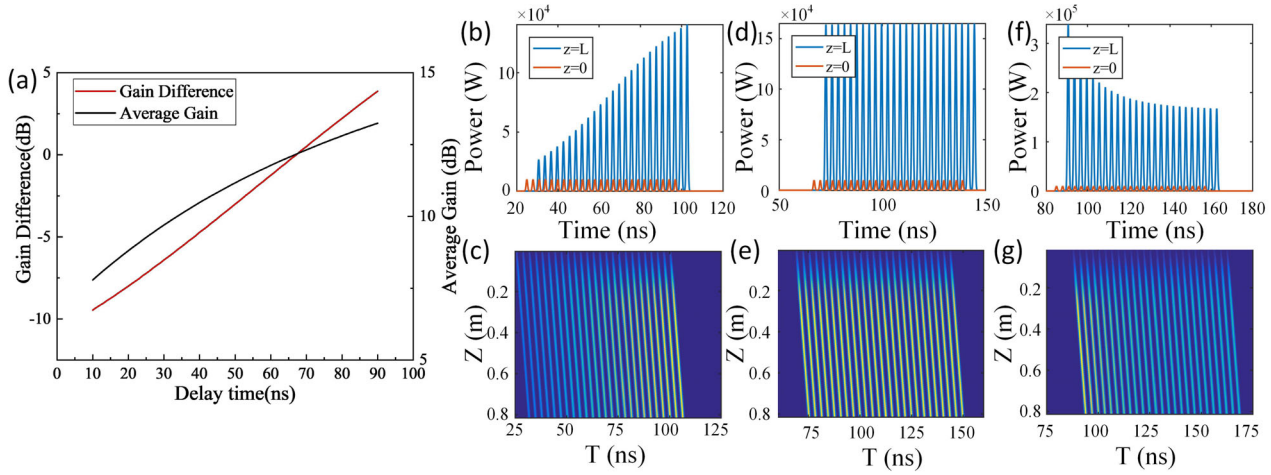

Fig.3 (a) Gain difference and average gain under different delay time; The pulse burst amplification with delay time of (b), (c) 25 ns, (d), (e) 67 ns and (f), (g) 85 ns

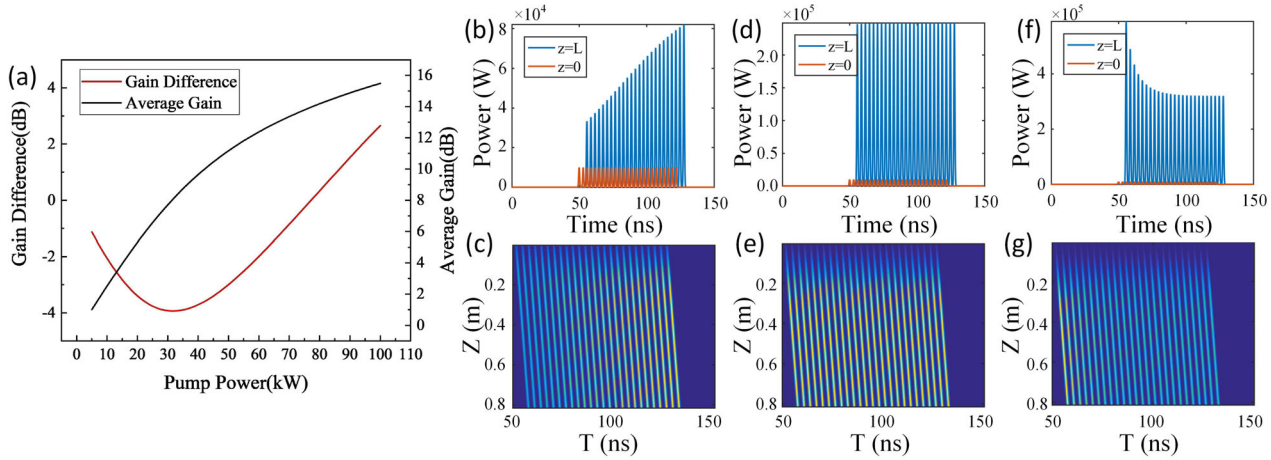

Fig.4 (a) Gain difference and average gain under different pump power; The pulse burst amplification with pump power of (b), (c) 30 kW, (d), (e) 77 kW and (f), (g) 100 kW

The output pulse energy and the stacking efficiency evolution under different gain difference caused by changing the signal delay time with pump power of 30 kW, 50 kW and 80 kW is plotted in Fig.5. As shown in Fig.5(a), with a fixed pump power, the output pulse energy increases with the increase of gain difference. As shown in Fig.5(b), the change trend of stacking efficiency caused by gain differences caused by signal delay time at different pump powers is consistent. The stacking efficiency is highest when the gain difference is less than 0 dB, because when the first pulse is incident into the GTI cavity, there is no coherent interference between it and pulse in the cavity, so that part of the first pulse energy is directly reflected out of the cavity. When the gain difference is slightly less than 0 dB, that is, the pulse energy at the front edge pulse of the burst is slightly lower than other pulses, the stacking efficiency is the highest. Therefore, although the pulse energy is increasing with the increase of gain difference, if the front edge pulse intensity of the pulse burst is too high, the residual pulse energy near the output pulse after stacking will be high.

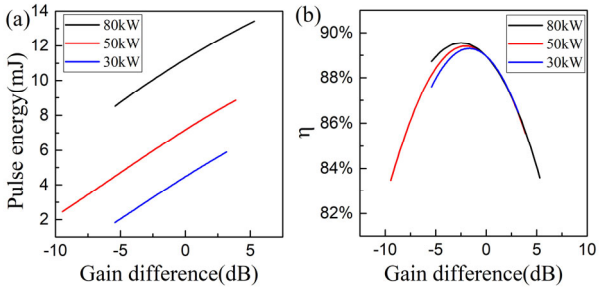

Fig.5 Variations in (a) output pulse energy and (b) stacking efficiency under different gain differences

In conclusion, the dynamic characteristics of the pulse burst in YDFA using high-power pulse pump are investigated in detail by a FDTD method. We analyze the average gain and the amplitude uniformity of the amplified pulse burst under different delay time and different pump power and duration. The results show that the amplifier can achieve a pulse burst with good amplitude uniformity by adjusting the signal delay time and the pump parameters. Then, the amplitude uniformity of the amplified pulse burst is considered to improve the output pulse energy and the efficiency of coherent pulse stacking. The output pulse with high efficiency and high pulse energy can be obtained by reasonably balancing the pulse pump power and signal delay time. It provides a theoretical basis for the design of fiber amplifier in coherent pulse stacking system.

References

[1] A. Klenke, M. Müller, H. Stark, M. Kienel, C. Jauregui, A. Tünnermann and J. Limpert, IEEE Journal of Selected Topics in Quantum Electronics **24**, 1 (2018).

[2] W. Yuan, Y. Jian-Quan, Z. Yi-Bo, W. Wu-Qi, L. U. Ying and W. J. O. L. Peng, Optoelectronics Letters **8**, 426 (2012).

[3] H. Kalaycioglu, K. Eken and F. Ö. İlday, Optics Letters **36**, 3383 (2011).

[4] S. Breitkopf, A. Klenke, T. Gottschall, H.-J. Otto, C. Jauregui, J. Limpert and A. Tünnermann, Optics Letters **37**, 5169 (2012).

[5] H. Kalaycıoğlu, Y. B. Eldeniz, Ö. Akçaalan, S. Yavaş, K. Gürel, M. Efe and F. Ilday, Optics Letters **37**, 2586 (2012).

[6] C. Kerse, H. Kalaycıoğlu, P. Elahi, Ö. Akçaalan and F. Ö. Ilday, Optics Communications **366**, 404 (2016).

[7] M. Nie, X. Cao, Q. Liu, E. Ji and X. Fu, Optics Express **25**, 13557 (2017).

[8] Y. Liu, J. Wu, X. Wen, W. Lin, W. Wang, X. Guan, T. Qiao, Y. Guo, W. Wang and X. Wei, Optics Express **28**, 13414 (2020).

[9] H. Kalaycıoğlu, Ö. Akçaalan, S. Yavaş, Y. B. Eldeniz and F. Ö. Ilday, Journal of the Optical Society of America B **32**, 900 (2015).

[10] H. Yu, Y. Qi, J. Zhang, S. Zou, L. Zhang, C. He, H. Chen, B. Li and X. Lin, IEEE Journal of Selected Topics in Quantum Electronics **24**, 1 (2017).

[11] C. Kerse, H. Kalaycıoğlu, P. Elahi, B. Çetin, D. K. Kesim, Ö. Akçaalan, S. Yavaş, M. D. Aşık, B. Öktem and H. Hoogland, Nature **537**, 84 (2016).

[12] T. Liu, J. Wang, G. I. Petrov, V. V. Yakovlev and H. F. J. M. P. Zhang, Medical Physics **37**, 1518 (2010).

[13] M. Murakami, B. Liu, Z. Hu, Z. Liu and Y. J. A. P. E. Che, Applied Physics Express **2**, 042501 (2013).

[14] K. Nagashima, Y. Ochi and R. Itakura, Optics Letters **45**, 674 (2020).

[15] T. Zhou, J. Ruppe, C. Zhu, I. N. Hu, J. Nees and A. Galvanauskas, Optics Express **23**, 7442 (2015).

[16] J. Ruppe, S. Chen, Z. Tong, M. Sheikhsofla and A. Galvanauskas, Coherent Pulse Stacking Extension of CPA to 9ns Effectively-Long Stretched Pulse Duration, Conference on Lasers and Electro-Optics, SM4I.2 (2016).

[17] H. Pei, J. Ruppe, S. Chen, M. Sheikhsofla, J. Nees, Y. Yang, R. Wilcox, W. Leemans and A. Galvanauskas, 10mJ Energy Extraction from Yb-doped 85μm core CCC Fiber using Coherent Pulse Stacking Amplification of fs Pulses, Advanced Solid State Lasers, AW4A.4 (2017).

[18] X. Yilun, W. Russell, B. John, D. Lawrence, D. Qiang, H. Gang, Y. Yawei, Z. Tong, L. Wim and R. John, IEEE Journal of Quantum Electronics **54**, 1 (2018).

[19] Y. Yawei, D. Lawrence, G. Almantas, D. Qiang, H. Gang, R. John, Z. Tong, W. Russell and L. Wim, Journal of the Optical Society of America B **35**, 2081 (2018).

[20] S. Yılmaz, P. Elahi, H. Kalaycıoğlu and F. Ö. Ilday, Journal of the Optical Society of America B **32**, 2462 (2015).

[21] H. T. Hattori and A. Khaleque, Applied Optics **55**, 1649 (2016).

[22] J. Boullet, R. Dubrasquet, C. Médina, R. Bello-Doua and E. Cormier, Optics Letters **35**, 1650 (2010).